Clinical value of routine use of thin-section 3D MRI using 3D FSE sequences with a variable flip angle technique for internal derangements of the knee joint at 3T

Hideyasu Kudo[a], Tsutomu Inaoka[a,*], Noriko Kitamura[a], Tomoya Nakatsuka[a] Shusuke Kasuya[a], Rumiko Kasai[a], Mitsuyuki Tozawa[b], Koichi Nakagawa[c], Hitoshi Terada[a]

[a] Department of Radiology, Toho University Sakura Medical Center, Sakura, Japan

[b] Division of Radiologic Technology, Toho University Sakura Medical Center, Sakura, Japan

[c] Department of Orthopaedic Surgery, Toho University Sakura Medical Center, Sakura, Japan

Abstract

Purpose

To determine the clinical value of routine use of thin-section 3D MRI using 3D FSE sequences with a variable flip angle technique for internal derangements of the knee joint at 3 T.

Method and Materials

Thirty-four knees in 34 patients suspected of having internal derangements of the knee joint were included. Following standard 2D MRI protocol including sagittal PDWI, T1WI and T2*WI, coronal fat-suppressed PDWI, and axial fat-suppressed PDWI with 3-4 mm thicknesses, fat-suppressed and water-excitation PDWI using 3D FSE sequences with a variable flip angle technique with 0.6 mm thickness were obtained in coronal plane and the three major planes with 1 mm thickness (3D MRI) was reformatted. The standard 2D MRI protocol and reformatted 3D MRI protocol (three sagittal 2D sequence images plus 3D MRI) were independently analyzed by two radiologists concerning presence or absence of lesions in the menisci, cartilage, and ligament. Interobserver agreements in both the MRI protocols were assessed by weighted-kappa coefficients. Regarding diagnostic accuracy, areas under the receiver operating characteristic curves (Az values) of both the MRI protocols were compared.

Results

Thirty-eight meniscal lesions, 39 cartilage lesions, and 20 ligamentous lesions were surgically detected. Excellent interobserver agreements (kappa = 0.91–0.98) were seen in both the MRI protocols, with a slightly better tendency in the reformatted 3D MRI protocol. Average Az values in detection of the meniscal, cartilage, and ligamentous lesions were significantly higher in the reformatted 3D MRI protocol than in the standard 2D MRI protocol ($p < 0.01$ or $p < 0.001$).

Conclusion

Routine use of reformatted thin-section 3D MRI using 3D FSE sequences with a variable flip angle technique may improve diagnostic accuracy and confidence in detection of internal derangements of the knee joint.

Keywords

MRI; 3 T; Three-dimensional; Fast spin echo; Knee

Introduction

Different three-dimensional (3D) sequences have recently been proposed in routine musculoskeletal magnetic resonance imaging (MRI). In knee MRI, currently, gradient-echo (GRE) sequences have predominantly been used in the 3D sequences [1–5]. The 3D GRE sequences have been very useful for assessing cartilage abnormalities, but they are less accurate than two-dimensional (2D) fast spinecho (FSE) sequences for assessing meniscus or ligaments [1–5]. Therefore, 3D FSE sequences have been attempted for comprehensive joint imaging, but a quite long imaging time has been a major disadvantage in conventional 3D FSE sequences. With the use of 3 T MRI systems, multichannel coils, and parallel imaging technique, images have been acquired with isotropic voxels in a shorter imaging time. By using 3 T MRI systems, however, high specific absorption rate (SAR) is a critical issue. With using a new variable flip angle technique, SAR can be reduced even at 3 T [6,7]. So far, 3D FSE sequences with a variable flip angle technique have now been attracted attention in comprehensive assessment of joint imaging at 3 T [1,8,9]. The primary advantages of imaging using 3D FSE sequences with a variable flip angle technique for knee MRI are the ability to obtain submillimeter contiguous slices with higher signal-to-noise ratio (SNR) and to generate isotropic images reformatted into various planes of better image contrast [1,8,9]. Therefore, 3D FSE sequences with a variable flip angle technique have been expected to be useful for the detection of smaller intraarticular lesions or for the preoperative planning by using postprocessing, highly resolved isotropic 3D MRI. Many preliminary studies comparing diagnostic efficacies of isotropic 3D MRI using 3D FSE sequences with a variable flip angle technique versus standard 2D MRI of the knee at 3 T have been done, and the diagnostic efficacies for internal derangements of the knee joint between them are reportedly the same [8,10–13]. In clinical practice, however, it is reasonable that a 3D FSE sequence with a variable flip angle technique is combined with several standard 2D sequences for the knee joint since a single of the 3D FSE sequence may not be thought to replace all the 2D sequences. To our knowledge, there is no study simply assessing clinical value of reformatted thin-section 3D MRI using 3D FSE sequence with a variable flip angle technique in routine MRI examinations for internal derangements of the knee joint at 3 T. The purpose of this study was to determine the clinical value of routine use of thin-section 3D MRI using 3D FSE sequences with a variable flip angle technique for internal derangements of the

knee joint at 3 T.

Materials and methods

Patient sample

The institutional review board in our hospital approved this study. Informed consent was obtained for the limited use of MRI data without the disclosure of any patients' information. The addition of 3D FSE sequence with a variable flip angle technique was approved since it has already been commercially available and total examination time is within the MRI examination time prescribed in our hospital. There were 352 consecutive patients suspected of knee abnormalities who underwent MRI in our hospital from October 2011 to July 2012. Patients with rheumatoid arthritis, septic arthritis, and tumors were excluded since such patients needed contrast enhanced MRI sequences. Patients with severe osteoarthritis (Kellegan-Lawrence grade 4 on the knee radiographs) were excluded since their cartilages or meniscus might be severely destructed. Patients who had undergone surgery involving the implantation of metal hardware around the knee joint were also excluded since metallic artifacts might reduce the diagnostic performance. Finally, 34 knees in 34 patients who underwent optimal standard 2D sequences and a 3D FSE sequence with variable flip angle technique at 3 T and whom diagnoses were surgically confirmed in our hospital were included in this study. All the patients were Asian population. There were 21 male and 13 female patients (mean age ± standard deviation, 46.5 ± 23.4 years; age range, 11–85 years). Twenty patients involved the right knee and 14 involved the left knee. The mechanisms of injury were sport-related injury in 15 patients, degenerative change (knee pain) in 12 patients, fall in three patients, motor vehicle accident in one patient, and other trauma in three patients. MRI All imaging was performed by a 3 T MR scanner (Magnetom Skyra, Siemens Medical Solution, Enlargen, Germany) with a 15-channel knee coil (TxRx, Quality Electrodynamics, Ohio, USA). The imaging protocol consisted of five 2D sequences and a single 3D FSE sequence with a variable flip angle technique with the parameters shown in Table 1. As 3D FSE sequence with a variable flip angle technique, 3D sampling perfection with application-optimized contrasts using different flip-angle evolutions (SPACE) sequence was used. The 2D sequence protocol consisted of sagittal 2D FSE proton density-weighted, 2D FSE T1-weighted, and 2D GRE T2*-weighted sequences, coronal fat-suppressed 2D FSE proton density-weighted sequence,

and axial fat-suppressed 2D FSE proton density-weighted sequence. The imaging time of the five 2D sequence protocol was 7 min 24 sec. The 3D sequence protocol consisted of a single fat suppressed 3D FSE proton density-weighted sequence in the coronal plane using SPACE 3D FSE sequences with a variable flip angle technique. Water-excitation technique was also added to increase the signal intensity in intraarticular fluid. The imaging times were 5 min 21 sec through 6 min 20 sec, which varied depending on the size of the knee joint. Therefore, the total imaging times including all the 2D and 3D sequences were 12 min 45 sec through 13 min 44 sec. Reformatted 3D MRI protocol was determined as three sagittal 2D sequences plus a 3D FSE sequence with a variable flip angle technique, and the estimated imaging times were from 10 min 22 sec to 11 min 11 sec.

Review of MR images

Images from all 34 knee MRI examinations were evaluated on a 2- monitor system and workstation in our intradepartmental picture archiving and communication system (PACS) network (Rapideye station; Toshiba Medical System, Japan). All images were stripped of identifying information. In 3D MRI, three major image planes (sagittal, coronal, and axial planes) with 1 mm thickness were reformatted from the source images of SPACE sequence with 0.6 mm thickness on the PACS workstation. As the readers needed, multiplanar images were freely reformatted on the PACS workstation and the slice thickness could be varied from 0.6 mm to 2 mm. Standard 2D MRI and reformatted 3D MRI protocols of the knee were independently reviewed by two radiologists (14 years and 4 years of experience). The reading of standard 2D MRI protocol was followed by the reading of reformatted 3D MRI protocol. These images were analyzed with regard to the presence or absence of lesions in the meniscus, cartilage, and ligaments. Regarding the meniscal lesions, type [vertical tear (longitudinal tear, radial tear, and oblique tear), horizontal tear, complex tear] and location (medial meniscus and lateral meniscus; anterior horn, body, posterior horn, root) of the lesions were recorded. Bucket-handle tears were categorized in the longitudinal tears. In the meniscal and ligamentous lesions, mucoid degeneration was excluded. The cartilage lesions were categorized as lesions at the medial femorotibial joint, lateral femorotibial joint, or patellofemoral joint, and the ligamentous lesions were categorized as lesions of the cruciate or collateral ligaments. Cartilage lesions were diagnosed by using the modified Outerbridge

grading system (grade 0 = normal; grade 1 = abnormal signal without a contour defect; grade 2 = contour defect less than or equal to 50% of cartilage thickness; grade 3 = contour defect greater than 50% of cartilage thickness; grade 4 = full-thickness contour defect with a subjacent signal abnormality in bone) [14]. So far, grade 2–4 cartilage lesions were included as positive findings in this study. The ligamentous lesions included complete and partial tears. In addition, a six-point stratification of the confidence level was used to grade these abnormalities: 1, definite absence of abnormality; 2, probably no presence of abnormality; 3, possibly no presence of abnormality; 4, possibly presence of abnormality; 5, probably presence of abnormality; and 6, definite presence of abnormality.

Standard of reference

The standard of reference was based on arthroscopic findings in 23 patients and arthrotomy findings in 11 patients. Arthroscopic and arthrotomy findings were recorded by one experienced orthopaedic surgeon. The interval period between MRI examination and arthroscopy or arthrotomy was 28.0 ± 24.3 days (range, 1–89 days).

Statistical analysis

For the six-point stratification of confidence level in the meniscal, cartilage, and ligamentous abnormalities from each patient, weighted kappa statistics were used to measure the level of agreement between the two readers in standard 2D MRI and reformatted 3D MRI protocols, respectively. A kappa value greater than 0 was considered to indicate a positive correlation in the following increments: 0.01–0.20, slight agreement; 0.21–0.40, fair agreement; 0.41–0.60, moderate agreement; 0.61–0.80, substantial agreement; and 0.81–1.00, excellent agreement [15]. To test the clinical value of routine use of reformatted thin-section 3D MRI using 3D FSE sequence with a variable flip angle technique, sensitivity, specificity, and accuracy of the standard 2D MRI and reformatted 3D MRI protocols for each lesion were calculated (positive at confidence level 4–6 and negative at confidence level 1–3). In addition, to test the diagnostic accuracy between the standard 2D MRI and reformatted 3D MRI protocols, areas under the receiver operating characteristic (ROC) curves (AUCs) (Az values) were calculated and compared in diagnosing the presence or absence of meniscal, cartilage, and ligamentous lesions. According to the location of lesions in the

meniscus, cartilage, or ligaments, sensitivity, specificity, accuracy, and Az value were also calculated. ROC analyses were performed using ROCKIT produced by Chicago University. Student's t-test was used for the statistical analyses. A p-value less than 0.05 was considered to represent a statistically significant difference.

Results

As a standard of reference, 38 meniscal lesions, 39 cartilage lesions, and 20 ligamentous lesions were surgically detected. Among the 38 meniscal lesions, 24 were in the medial meniscus and 14 were in the lateral meniscus. They consisted of 13 vertical tears, seven horizontal tears, and 18 complex tears. Regarding the cartilage lesions, 15 lesions were at the medial femorotibial joint, nine were at lateral femorotibial joint, and 15 were at patellofemoral joint. They consisted of 14 grade 2, 15 grade 3, and 10 grade 4 cartilage lesions. These are summarized in Tables 2 and 3. Regarding the ligamentous lesions, 14 were in the anterior cruciate ligament, one was in the posterior cruciate ligament, and five were in the medial collateral ligament. All the ligamentous lesions were complete tears. The interobserver agreement (kappa values) in determining presence or absence of the lesions in the meniscus, cartilage, and ligaments in the standard 2D MRI and reformatted 3D MRI protocols were shown in Table 4. Although excellent interobserver agreements were seen in both the standard 2D MRI and reformatted 3D MRI protocols, except for cartilage lesions at the lateral femorotibial joint, those of the reformatted 3D MRI protocol were slightly better than those of the standard 2D MRI protocol. Sensitivity, specificity, and accuracy of the standard 2D MRI and reformatted 3D MRI protocols were shown in Table 5. The results of ROC analyses are summarized in Table 6. Average Az values of two readers in detection of all the lesions were statistically better in the reformatted 3D MRI protocol than in the standard 2D MRI protocol ($p < 0.01$ or $p < 0.001$). Representative cases are shown in Figs. 1 through 5.

Discussion

Several preliminary studies using new 3D FSE sequences with a variable flip angle technique for knee MRI at 3 T have been reported. Most investigators said that reformatted 3D MRI using 3D FSE sequences with a variable flip angle technique was almost equal to standard MRI with 2D sequences in multiple planes in detecting meniscal, cartilage, and ligamentous lesions of the knee joint

[8,10–13]. The slice thicknesses were usually 2 mm, but in our study, we used 3D reformation with 1 mm thickness. It was elucidated that the integration of reformatted thin-section 3D MRI using 3D FSE sequences with a variable flip angle technique to routine MRI examination may actually improve diagnostic accuracy and confidence in detection of internal derangements of the knee joint at 3 T. Regarding the meniscal lesions, a study performed by Subhas et al. [13] described that reformatted 3D MRI using SPACE sequence was inferior to standard 2D MRI in the detection of meniscal lesions. Particularly in assessing medial meniscal tears, reformatted 3D MRI using SPACE sequence was worse than standard 2D MRI, but in terms of lateral meniscal tear, the results of 2D MRI and 3D MRI using SPACE sequence were equal. In our results, thin-section 3D MRI using SPACE sequence was very useful in detection of meniscal lesions as well as most of the other previous reports. We consider that contiguous thin-section 3D MRI with 3D FSE sequences with a variable flip angle technique is very valuable in assessing meniscal tears independent of the location. In the Subhas's study, a relatively shorter repetition time (TR) and a longer echo time (TE) were used. Then, the setting of TR and TE might greatly influence the image contrast weighting in 3D FSE sequence with a variable flip angle technique. Regarding the cartilage lesions, a study by Kijowski et al. using 3D FSE sequence with a variable flip angle technique (Cube 3D FSE, GE Healthcare) at 3 T described that 3D MRI using 3D FSE sequence with a variable flip angle technique was significantly more sensitive but less specific than standard 2D MRI for the detection of cartilage abnormalities [10]. In Notohamiprodjo's study using SPACE sequence [8], there were no significant differences between standard 2D MRI and reformatted 3D MRI in detection of cartilage abnormalities. In our results, reformatted thin-section 3D MRI using SPACE sequence was much more valuable for the detection of smaller cartilage lesions compared to standard 2D MRI. We consider that contiguous thin-section images in multiple planes were very useful in assessment of cartilage abnormalities at the convex-shaped femoral condyle and patella and the concave-shaped trochlea. In addition, it has previously been reported that slightly lower contrast between the cartilage and intraarticular fluid in 3D FSE sequences [1,16]. Therefore, we added water-excitation technique to increase the signal intensity of intraarticular fluid and contrast between intraarticular fluid and cartilage in this study. Longer imaging time is still a great disadvantage of 3D FSE sequences. Estimated imaging time of reformatted 3D MRI protocol was

about 2–3 minutes longer than those of standard 2D MRI protocol in this study. With using of 3 T MRI, parallel imaging technique, and 15-channel knee coil, the imaging time of standard 2D MRI protocol was also much shorter than before. However, we believe that the integration of contiguous thin-section 3D MRI using 3D FSE with a variable flip angle technique to routine MRI examination is potentially valuable for the detection of smaller intraarticular lesions of the knee joint. In actual, diagnostic accuracy and confidence to detect internal derangements of the knee joint were greatly improved in comparison with those of standard 2D MRI protocol in this study. So far, this improvement may compensate for the disadvantage of the longer imaging time of 3D FSE sequences at 3 T. There are some limitations in this study. First, a small number of patients with intraarticular abnormalities of the knee joint were enrolled. A larger series are warranted. Second, the image reading in this study was performed by only two readers with different experience. In the Subhas's study [13], six readers with various experience were used for assessing meniscal and ligamentous lesions. They reported a low to moderate correlation between the interpreting results and reader experience in both standard 2D MRI and SPACE sequence images. In our study, however, a slightly better tendency in interobserver agreement was seen in reformatted 3D MRI protocol than in standard 2D MRI protocol. Third, we used a proton-density weighted sequence with fat-suppression in 3D FSE sequence with a variable flip angle technique according to the previous studies [8,10–13]. However, it may be necessary to assess which sequence in 3D FSE sequence with a variable flip angle technique should be selected for the incorporation to routine MRI instead of several standard 2D sequences. In conclusion, we found that the integration of reformatted thin-section 3D MRI using 3D FSE sequence with a variable flip angle technique to routine MRI examination was very beneficial for the comprehensive assessment of the internal derangements of the knee joint at 3 T in clinical practice. As the main reason for this, we consider that 3D FSE sequence with a variable flip angle technique enables us to obtain submillimeter contiguous sections with higher SNR and the reformation of images into multiple planes with better image contrast. Longer imaging time is still a disadvantage of 3D FSE sequences, but the great improvement of diagnostic accuracy and confidence in detection of the internal derangements of the knee joint is considered to compensate for this weakness of the sequences.

References

1. Kijowski R, Gold GE. Routine 3D magnetic resonance imaging of joints. JMRI 2011;33:758–71.

2. Disler DG, McCauley TR, Kelman CG, Fucus MD, Ratner LM, Wirth CR, et al. Fatsuppressed three-dimensional spoiled gradient-echo MR imaging of hyaline cartilage defects in the knee: comparison with standard MR imaging and arthroscopy. AJR 1996;167:127–32.

3. Guckel C, Jundt G, Schnabel K, Gachter A. A spin-echo and 3D gradient-echo imaging of the knee joint: a clinical and histopathological comparison. Eur J Radiol 1995;21:25–33.

4. Duc SR, Pfirrmann CWA, Schmid MR, Zanetti M, Koch PP, Kalberer F, et al. Articular cartilage defects detected with 3D water-excitation true FISP: prospective comparison with sequences commonly used for knee imaging. Radiology 2007;245:216–23.

5. Kijowski R, Blankenbaker DG, Klaers JL, Shinki K, De Smet AA, Block WF. Vastly undersampled isotropic projection steady-state free precession imaging of the knee: diagnostic performance compared with conventional MR. Radiology 2009;251:185–94. [6] Busse RF, Hariharan H, Vu A, Brittain JH. Fast spin echo sequences with very long echo trains: design of variable refocusing flip angle schedules and generation of clinical T2 contrast. Magn Reson Med 2006;55:1030–7.

7. Busse RF, Brau AC, Vu A, Michelich CR, Bayram E, Kijowski R, et al. Effects of reforcusing flip angle modulation and view ordering in 3D fast spin echo. Magn Reson Med 2008;60:640–9.

8. Notohamiprodjo M, Horng A, Pietschmann MF, Muller PE, Horger W, Park J, et al. MRI of the knee at 3 T: first clinical results with an isotropic PDfs-weighted 3D-TSE-sequence. Invest Radiol 2009;44:585–97.

9. Friedrich KM, Reiter G, Kaiser B, Mayerhofer M, Deimling M, Jellus V, et al. Highresolution cartilage imaging of the knee at 3 T: basic evaluation of modern isotropic 3D MR-sequences. Eur J Radiol 2011;78:398–405.

10. Kijowski R, Davis KW, Woods MA, Lindstrom MJ, De Smet AA, Gold GE, et al. Knee joint: comprehensive assessment with 3D isotropic resolution fast spin-echo MR imaging – diagnostic performance compared with that of conventional MR imaging at 3.0 T. Radiology 2009;252:486–95.

11. Jung JY, Yoon YC, Kwon JW, Ahn JH, Choe BK. Diagnosis of internal derangement of the knee at 3.0-T MR imaging: 3D isotropic

intermediate-weighted versus 2D sequences. Radiology 2009;253:780–7.
12. Ristow O, Steinbach L, Sabo G, Krug R, Huber M, Rauscher I, et al. Isotropic 3D fast spin-echo imaging versus standard 2D imaging at 3.0 T of the knee – image quality and diagnostic performance. Eur Radiol 2009;19: 1263–72.
13. Subhas N, Kao A, Freire M, Polster JM, Obuchowski NA, Winalski CS. MRI of the knee ligaments and menisci: comparison of isotropic resolution 3D and conventional 2D fast spin-echo sequences at 3 T. AJR Am J Roentgenol 2011;197:442–50.
14. Uhl M, Allmann KH, Ihling C, Hauer MP, Conca W, Langer M. Cartilage destruction in small joints by rheumatoid arthritis: assessment of fat-suppressed threedimensional gradient-echo MR pulse sequences in vitro. Skeletal Radiol 1998; 27:677–82.
15. Kundel HL, Polansky M. Measurement of observer agreement. Radiology 2003; 228:303–8.
16. Gold GE, Busse RF, Beehler C, Han E, Brau AC, Beatty PJ, et al. Isotropic MRI of the knee with 3D fast spin-echo extended echo-train acquisition (XETA): initial experience. AJR Am J Roentgenol 2007;188:1287–93.

Table 1.
Parameters of MRI of the knee.

	2D MRI					3D MRI
Parameter	Sagittal 2D FSE PDWI	Sagittal 2D FSE T1WI	Sagittal 2D GRE T2*WI	Coronal 2D FSE FS PDWI	Axial 2D FSE FS PDWI	Coronal SPACE FS PDWI
TR (msec)	3500	520	700	2500	2500	1200
TE (msec)	30	11	16	11	11	15
FOV (cm)	16	16	16	16	16	16
Slice thickness (mm)	3-4	3-4	3-4	3-4	3-4	0.6
Matrix size	384 × 384	448 × 448	384 × 256	448 × 448	448 × 448	256 × 256 (512 × 512□)
Voxel size (mm)	0.4 × 0.4 × 3-4	0.4 × 0.4 × 3-4	0.4 × 0.4 × 3-4	0.4 × 0.4 × 3-4	0.4 × 0.4 × 3-4	0.6 × 0.6 × 0.6 (0.3 × 0.3 × 0.6□)
Turbo factor	12	2		6	6	70
Number of signal acquisition	2	1	1	1	1	1
Imaging time	1 min 36 sec	1 min 25 sec	1 min 50 sec	1 min 14 sec	1 min 19 sec	5 min 21 sec–6 min 20 sec

Note. 2D: two dimensional, 3D: three-dimensional, FS: fat-suppressed, FSE: fast spine echo, GRE: gradient-echo, SPACE: sampling perfection with application-optimized contrasts using

different flip-angle evolutions (3D FSE with a variable flip angle technique), PDWI: proton density-weighted image, TR: repetition time, TE: echo time, FOV: field of view.

- Interpolation.

Table 2.

Type and location of the 38 meniscal lesions.

	Medial meniscus	Lateral meniscus	Total
Vertical tear	7	6	13
Longitudinal tear	3	3	6
Radial tear	4	1	5
Oblique tear	0	2	2
Horizontal tear	2	5	7
Complex tear	15	3	18
Total	24	14	38

Table 3.
Grade and location of the 39 cartilage lesions.

	Medial femorotibial joint	Lateral femorotibial joint	Patellofemoral joint	Total
Grade 2	3	5	6	14
Grade 3	6	3	6	15
Grade 4	6	1	3	10
Total	15	9	15	39

Table 4.
Interobserver agreement with standard 2D MRI and reformatted 3D MRI protocols for determining presence or absence of internal derangements of knee joint.

	Protocol	
Lesions	Standard 2D MRI	Reformatted 3D MRI
All meniscus	0.94	0.95
Medial meniscus	0.96	0.98
Lateral meniscus	0.91	0.92
All cartilage	0.92	0.93
Medial femorotibial joint	0.93	0.95
Lateral femorotibial joint	0.93	0.92
Patellofemoral joint	0.92	0.93
All ligaments	0.94	0.97
Cruciate ligaments	0.93	0.96
Collateral ligaments	0.96	0.98

Note. Reformatted 3D MRI protocol: three sagittal 2D sequence images plus 3D MRI.

Table 5.
Sensitivity, specificity, and accuracy of standard 2D MRI and reformatted 3D MRI protocols in detection of internal derangements of knee joint.

	Sensitivity (%)		Specificity (%)		Accuracy (%)	
Lesions	Standard 2D MRI	Reformatted 3D MRI	Standard 2D MRI	Reformatted 3D MRI	Standard 2D MRI	Reformatted 3D MRI
Meniscus (n = 38)						
Reader 1	84.2(32/38)	86.8(33/38)	93.3(28/30)	96.7(29/30)	88.2(60/68)	91.2(62/68)
Reader 2	84.2(32/38)	84.2(32/38)	93.3(28/30)	96.7(29/30)	88.2(60/68)	89.7(61/68)
Average	84.2(64/76)	85.5(65/76)	93.3(56/60)	96.7(58/60)	88.2(120/136)	90.4(123/136)
Cartilage (n = 39)						
Reader 1	84.6(33/39)	89.7(35/39)	88.9(56/63)	96.8(61/63)	87.3(89/102)	94.1(96/102)
Reader 2	74.4(29/39)	82.1(32/39)	87.3(55/63)	92.1(58/63)	82.4(84/102)	88.2(90/102)
Average	79.5(62/78)	85.9(67/78)	88.1(111/126)	94.4(119/126)	84.8(173/204)	91.2(186/204)
Ligaments (n = 20)						
Reader 1	80.0(16/20)	85.0(17/20)	89.6(43/48)	91.7(44/48)	86.8(59/68)	89.7(61/68)
Reader 2	80.0(16/20)	90.0(18/20)	89.6(43/48)	93.8(45/48)	86.8(59/68)	92.6(63/68)
Average	80.0(32/40)	87.5(35/40)	89.6(86/96)	92.7(89/96)	86.8(118/136)	91.2(124/136)

Note. Reformatted 3D MRI protocol: three sagittal 2D sequence images plus 3D MRI.

Table 6.
ROC analyses (Az values) of standard 2D MRI and reformatted 3D MRI protocols in detection of meniscal, cartilage, and ligamentous lesions.

(a) Meniscal lesions

	Az value		
	Standard 2D MRI	Reformatted 3D MRI	p value
All meniscal lesions (n = 38)			
Reader 1	0.908 (0.834–0.981)	0.949 (0.897–1.000)	p < 0.001
Reader 2	0.894 (0.818–0.971)	0.910 (0.834–0.987)	NS
Average	0.902 (0.850–0.953)	0.931 (0.886–0.975)	p < 0.001
Medial meniscal lesions (n = 24)			
Reader 1	0.902 (0.793–1.000)	0.946 (0.871–1.000)	p < 0.001
Reader 2	0.927 (0.838–1.000)	0.933 (0.852–1.000)	NS
Average	0.914 (0.844–0.985)	0.940 (0.885–0.996)	p < 0.001
Lateral meniscal lesions (n = 14)			
Reader 1	0.895 (0.775–1.000)	0.946 (0.867–1.000)	p < 0.001
Reader 2	0.846 (0.707–0.986)	0.873 (0.736–1.000)	NS
Average	0.876 (0.786–0.966)	0.911 (0.833–0.990)	p < 0.001

(b) Cartilage lesions

	Az value		p value
	Standard 2D MRI	Reformatted 3D MRI	
All cartilage lesions (n = 39)			
Reader 1	0.917 (0.859–0.975)	0.965 (0.924–1.000)	p < 0.001
Reader 2	0.858 (0.777–0.938)	0.923 (0.865–0.982)	p < 0.001
Average	0.888 (0.841–0.935)	0.946 (0.914–0.978)	p < 0.001
Medial femorotibial joint (n = 15)			
Reader 1	0.897 (0.786–1.000)	0.923 (0.828–1.000)	NS
Reader 2	0.877 (0.750–1.000)	0.898 (0.788–1.000)	NS

(a) Meniscal lesions

	Az value		
	Standard 2D MRI	Reformatted 3D MRI	p value
Average	0.886 (0.801–0.972)	0.912 (0.841–0.983)	p < 0.001
Lateral femorotibial joint (n = 9)			
Reader 1	0.907 (0.761–1.000)	0.993 (0.976–1.000)	p < 0.001
Reader 2	0.778 (0.590–0.966)	0.922 (0.833–1.000)	p < 0.001
Average	0.839 (0.722–0.956)	0.961 (0.917–1.000)	p < 0.001
Patellofemoral joint (n = 15)			
Reader 1	0.947 (0.883–1.000)	0.993 (0.978–1.000)	p < 0.001
Reader 2	0.909 (0.804–1.000)	0.967 (0.901–1.000)	p < 0.001
Average	0.929 (0.864–0.993)	0.975 (0.940–1.000)	p < 0.001

(c) Ligamentous lesions

	Az value		p value
	Standard 2D MRI	Reformatted 3D MRI	
All ligamentous lesions (n = 20)			
Reader 1	0.938 (0.885–0.991)	0.940 (0.878–1.000)	NS
Reader 2	0.914 (0.829–1.000)	0.955 (0.900–1.000)	p < 0.001
Average	0.926 (0.876–0.975)	0.948 (0.906–0.991)	p < 0.001
Cruciate ligament lesions (n = 15)			
Reader 1	0.865 (0.737–0.993)	0.888 (0.779–0.997)	p < 0.05
Reader 2	0.898 (0.789–1.000)	0.916 (0.826–1.000)	NS
Average	0.881 (0.797–0.965)	0.903 (0.828–0.977)	p < 0.01
Collateral ligament lesions (n = 5)			
Reader 1	1.000 (1.000–1.000)	1.000 (1.000–1.000)	NS
Reader 2	0.886 (1.000–1.000)	1.000 (0.689–1.000)	p < 0.001
Average	0.942 (0.834–1.000)	1.000 (1.000–1.000)	p < 0.001

Note. Reformatted 3D MRI protocol: three sagittal 2D sequence images plus 3D MRI, NS: not statistically significant. 95% confidence intervals in parentheses.

Fig. 1.
A 14-year-old female with horizontal tear at the posterior horn of the medial meniscus. (A) Sagittal 2D FSE proton density-weighted image with 4 mm slice thickness, (B) axial fat-suppressed 2D FSE proton weighted-image with 4 mm slice thickness, (C) reformatted sagittal fat-suppressed 3D FSE proton-density weighted image with 1 mm slice thickness, and (D) reformatted axial fat-suppressed 3D FSE proton-density weighted image with 1 mm slice thickness. Horizontal tear at the posterior horn of the medial meniscus is shown more clearly on reformatted sagittal and axial 3D FSE images than on sagittal and axial 2D FSE images (arrows).

Fig. 2.
A 43-year-old male with longitudinal tear of the body through posterior horn of the medial meniscus. (A) Coronal fat-suppressed 2D FSE proton density-weighted image with 4 mm slice thickness, (B) axial fat-suppressed 2D FSE proton density-weighted image with 4 mm slice thickness, and (C) reformatted coronal, (D) sagittal, and (E) axial fat-suppressed 3D FSE proton density-weighted image with 1 mm slice thickness. Reformatted coronal, sagittal, and axial images more accurately show the extension of longitudinal tear of the medial meniscus. These findings are very valuable for preoperative planning.

Fig. 3.
A 36-year-old-male with a focal defect (grade 3) at the articular cartilage of the lateral femoral condyle. (A) Coronal fat-suppressed and (B) sagittal 2D FSE proton-density weighted image with 4 mm slice thickness, and (C) reformatted coronal and (D) sagittal fat-suppressed 3D FSE proton-density weighted images with 1 mm slice thickness. Reformatted coronal and sagittal 3D FSE images more clearly show a focal cartilage defect at the lateral femoral condyle, although coronal and sagittal 2D FSE images show a faint focal signal change at the articular cartilage of the lateral femoral condyle (arrows).

Fig. 4.
A 35-year-old female with a focal defect (grade 3) at the articular cartilage of the posterior aspect of the lateral femoral condyle. (A) Coronal, (B) axial fat-suppressed 2D FSE proton density-weighted image with 4 mm slice thickness, (C) reformatted oblique coronal and (D) oblique axial fat-suppressed

3D FSE proton density-weighted image with 1 mm slice thickness. On 3D FSE images, a focal defect is clearly visualized at the posterior aspect of the articular cartilage of the lateral femoral condyle (arrows). However, the finding of cartilage defect is unclear on 2D FSE images (arrows).

Fig. 5.
A 62-year-old female with complete tear of the anterior cruciate ligament. (A) sagittal 2D FSE proton density-weighted image, (B) sagittal 2D GRE T2*-weighted image with 4 mm slice thickness, and (C) reformatted sagittal fat-suppressed 3D FSE proton density-weighted image with 1 mm slice thickness. On sagittal 2D images, the anterior cruciate ligament shows an enlargement with high signal intensity (arrows), but complete disruption of the anteromedial bundle of the anterior cruciate ligament is seen on 3D FSE image (arrows). Therefore, the diagnosis of complete tear of the anterior cruciate ligament was determined with higher confidence on 3D FSE image than 2D images.

Fig 1A

Fig 1B

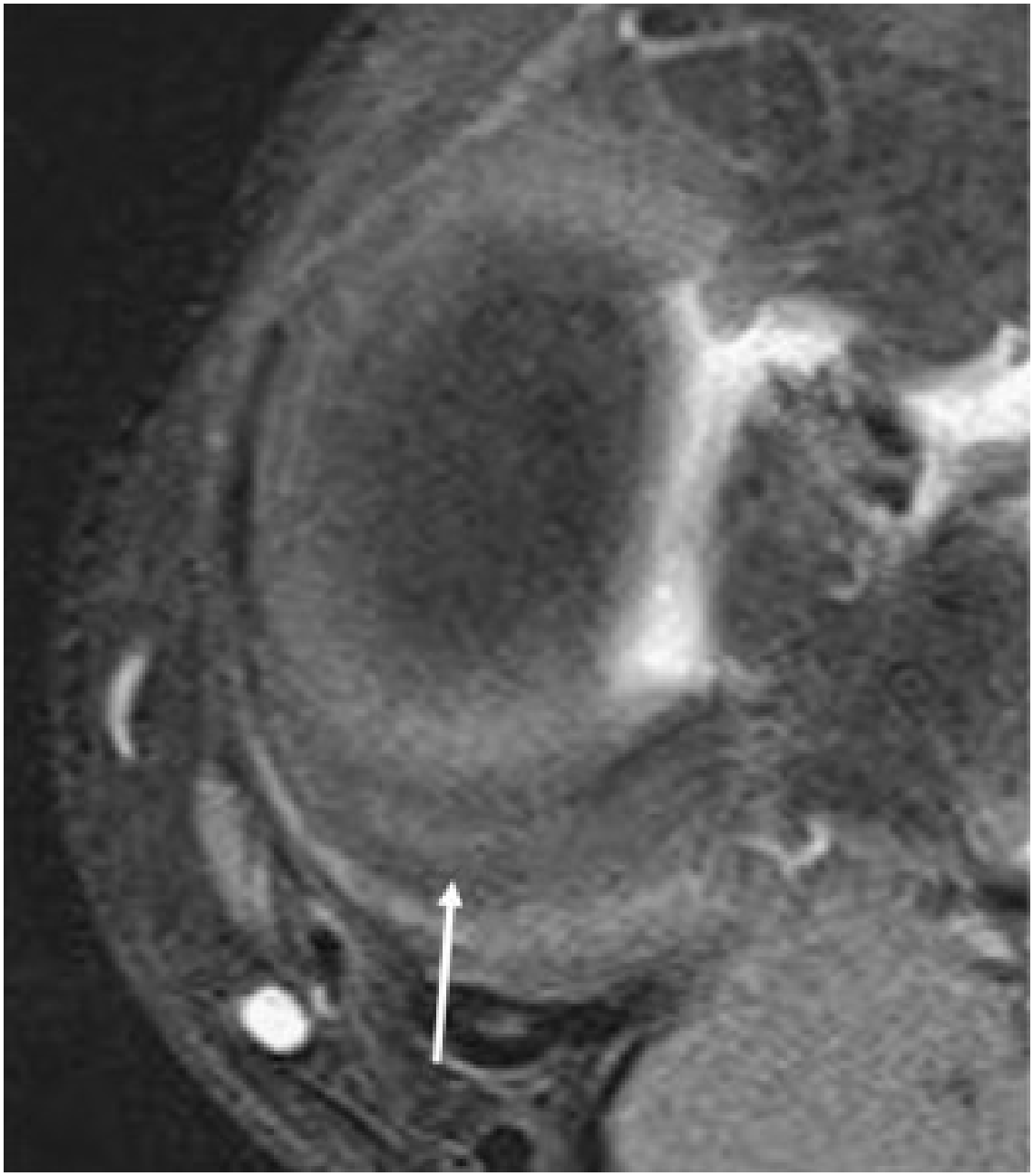

Fig 1C

Fig 1D

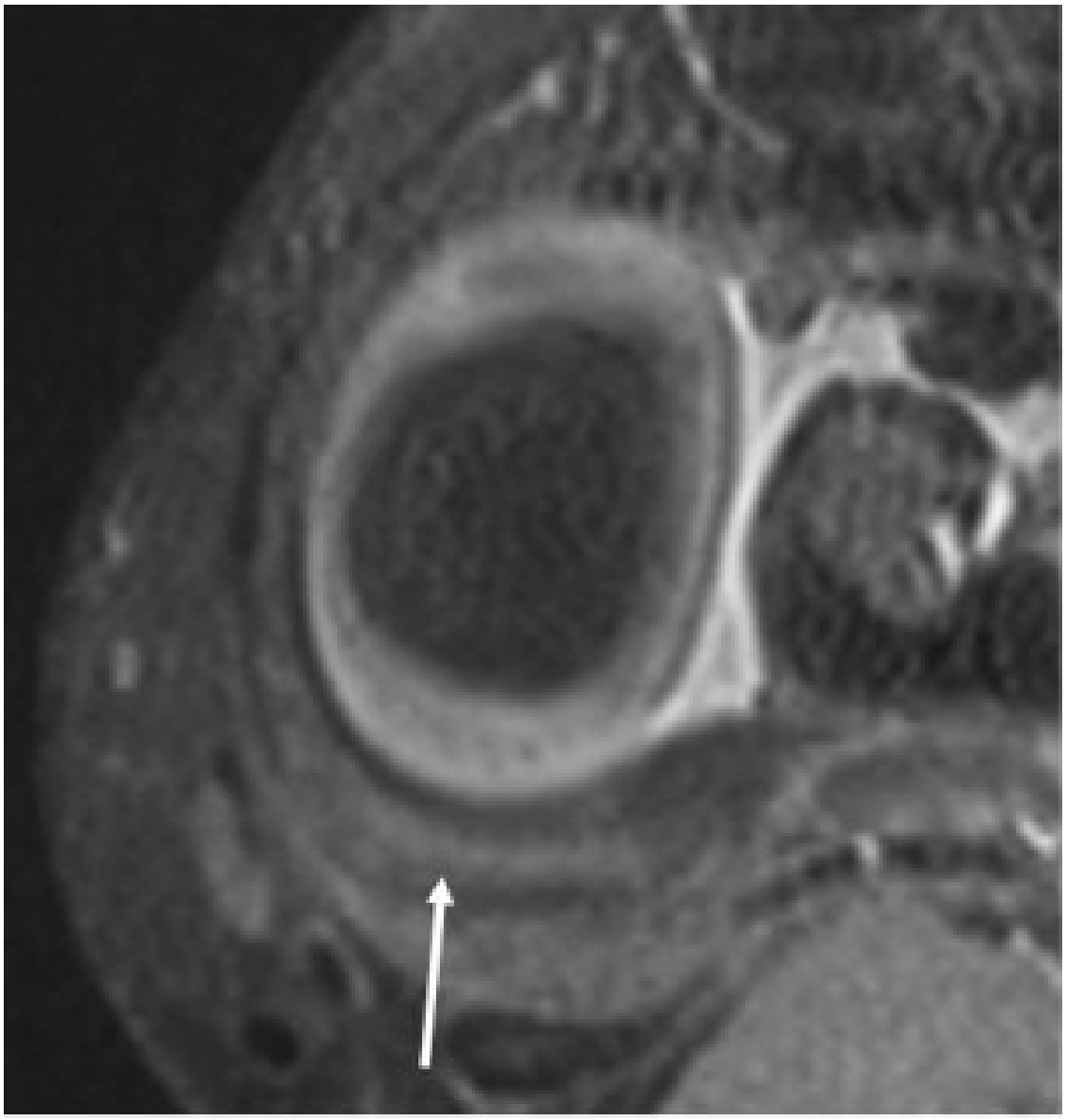

Fig 2A

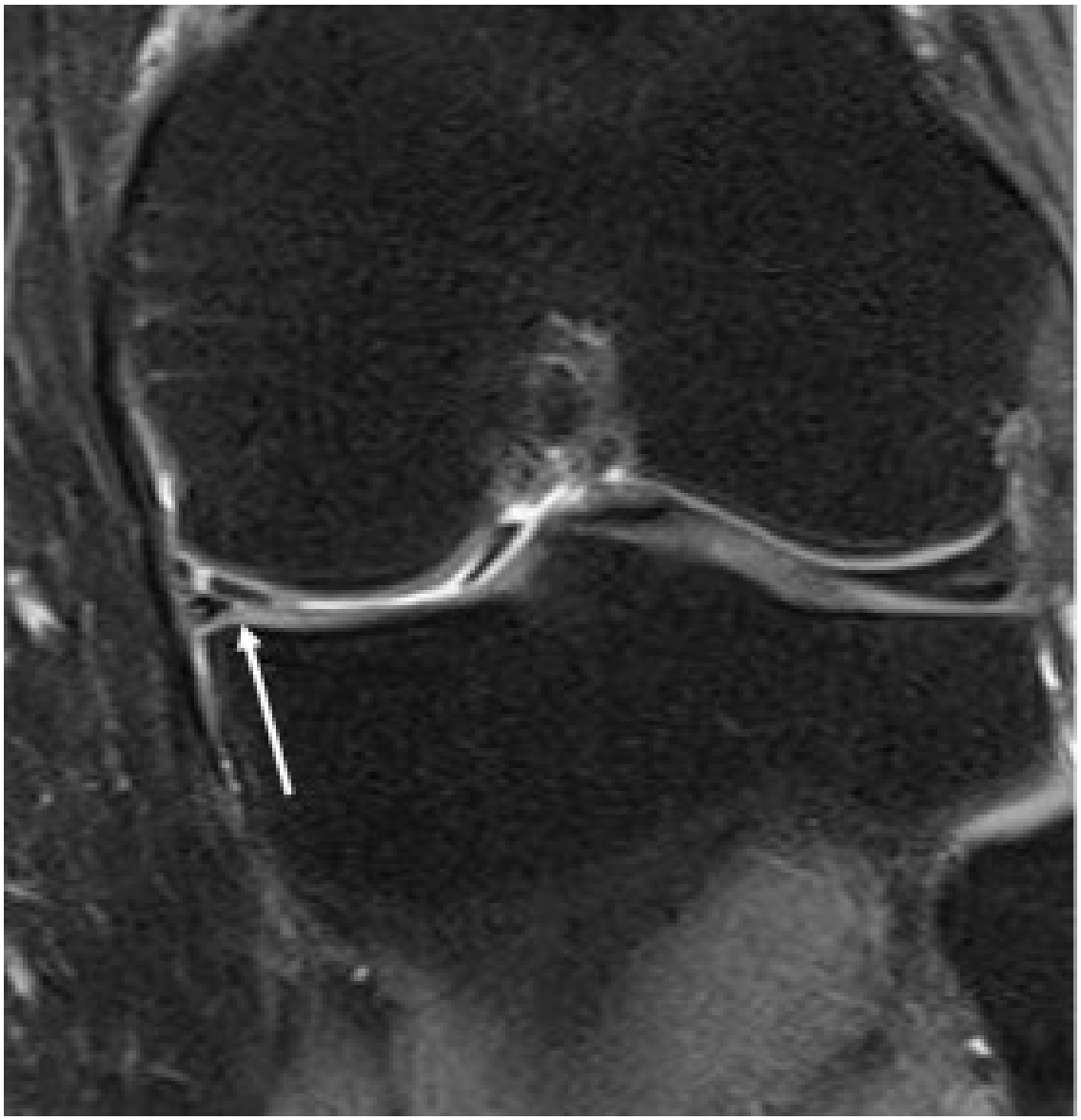

Fig 2B

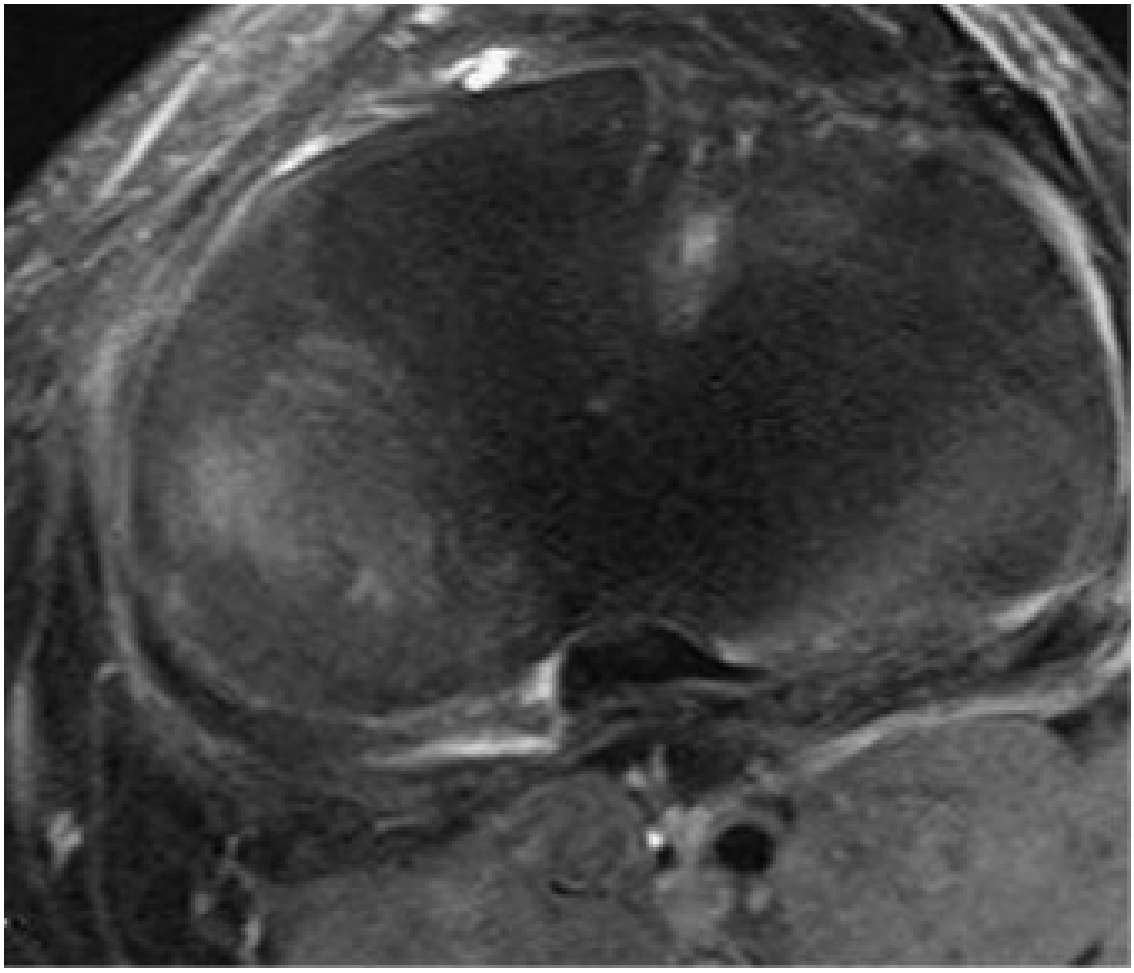

Fig 2C

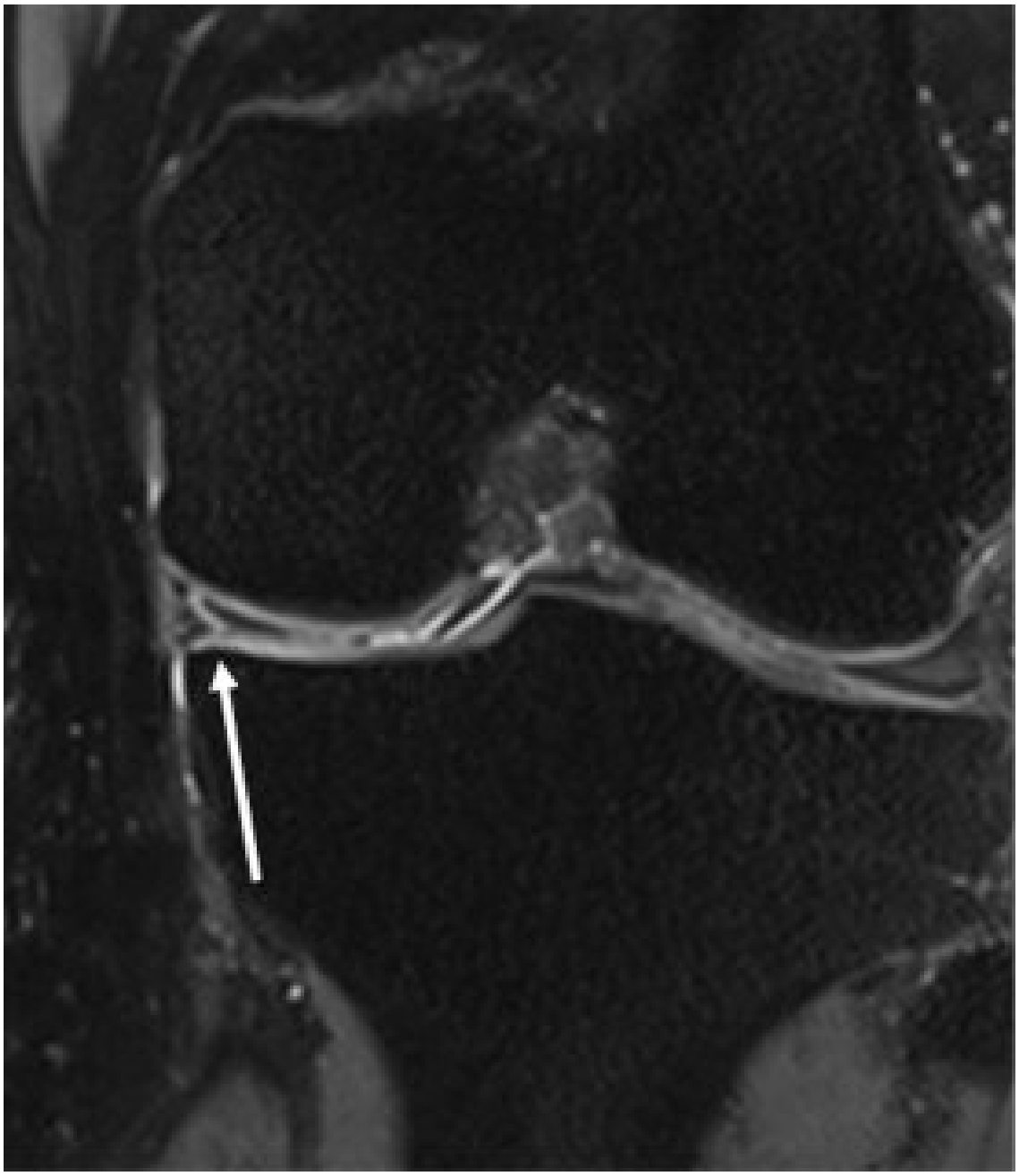

Fig 2D

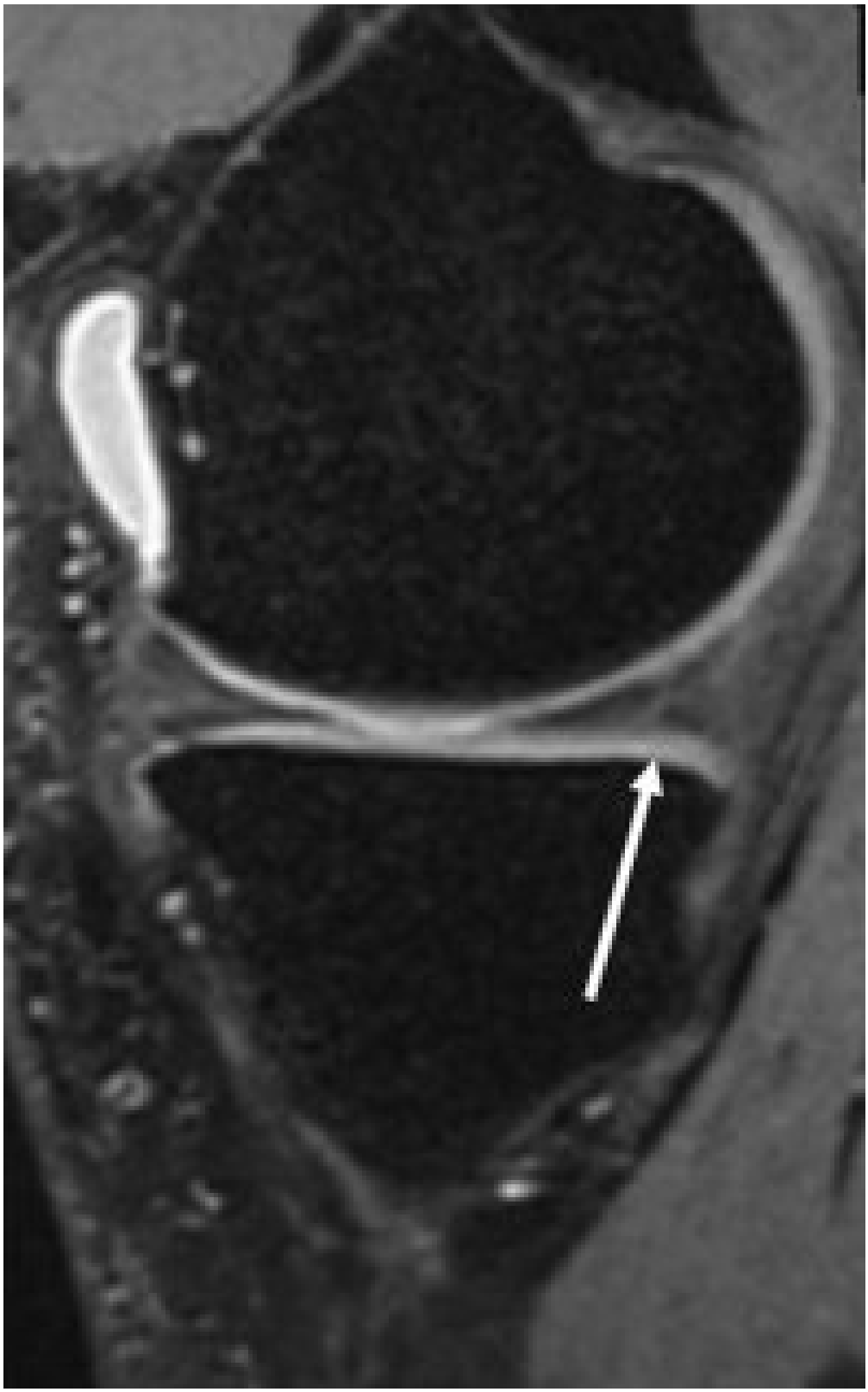

Fig 2E

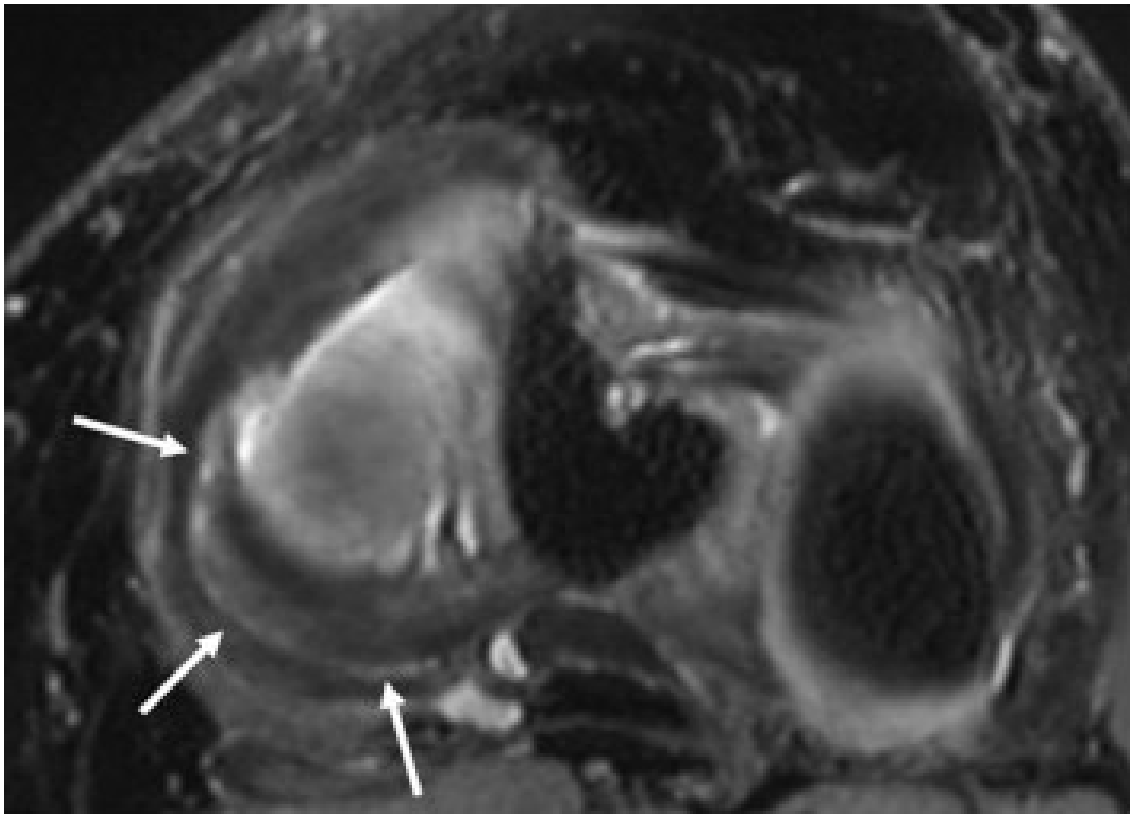

Fig 3A

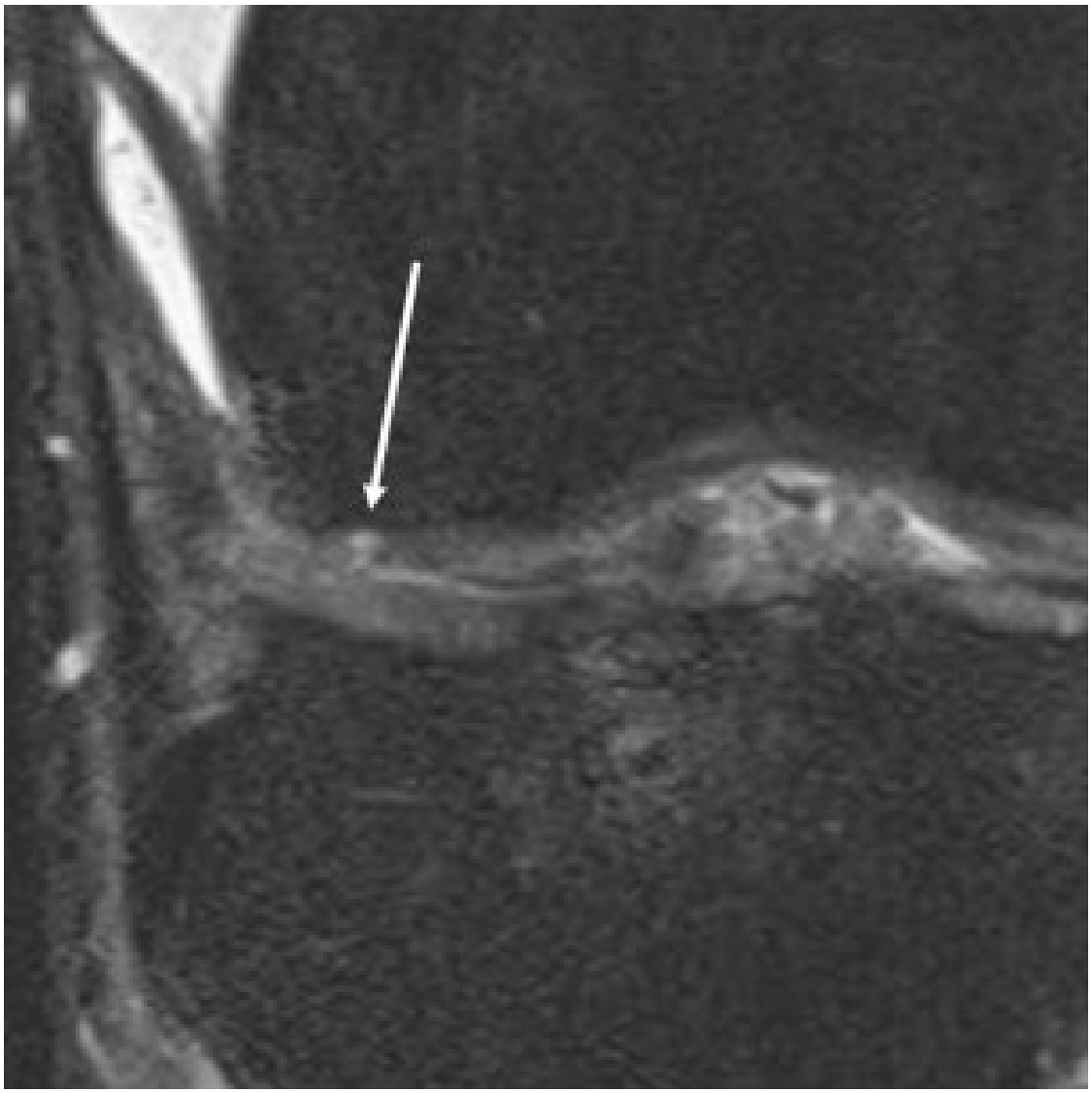

Fig 3B

Fig 3C

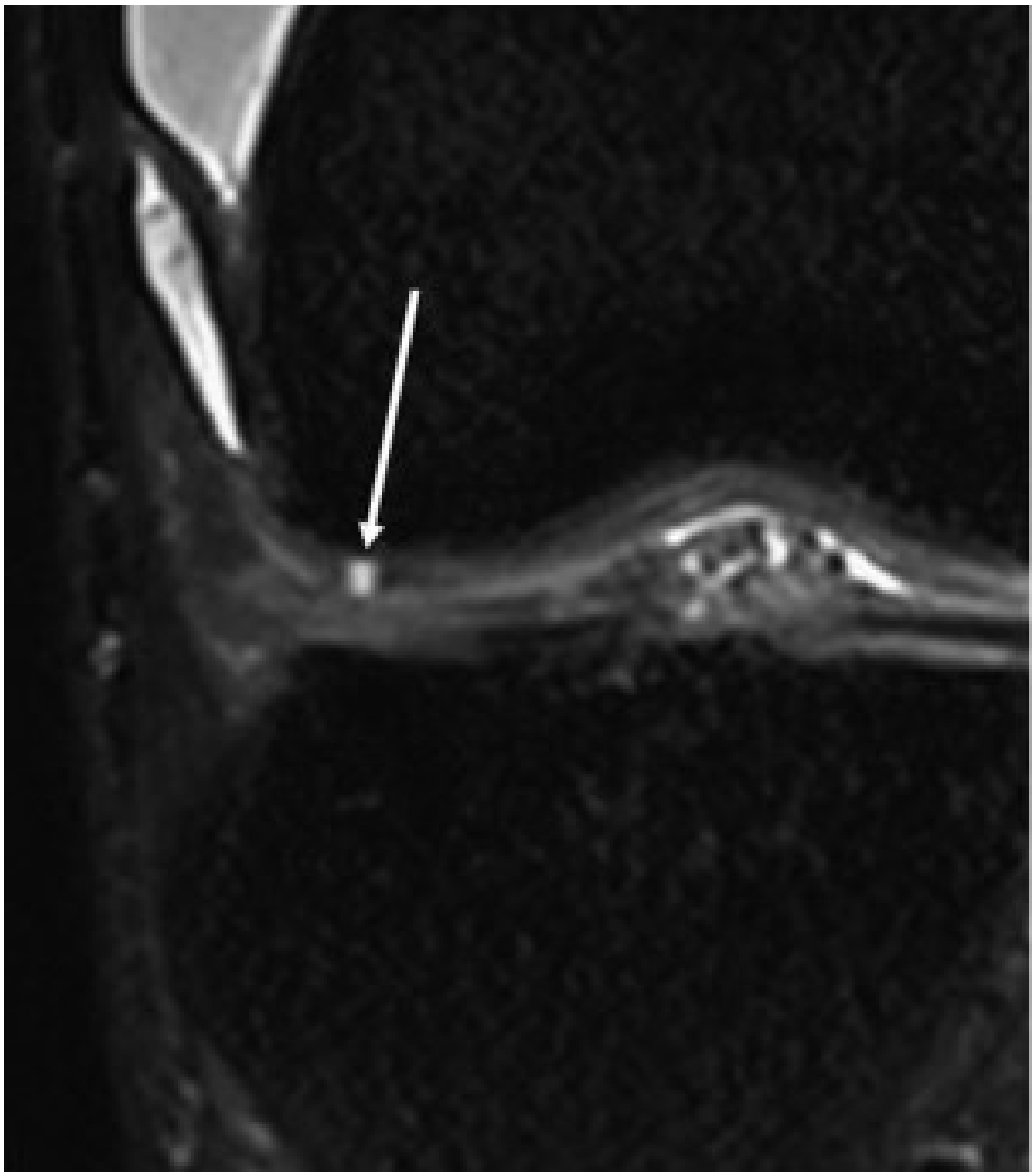

Fig 3D

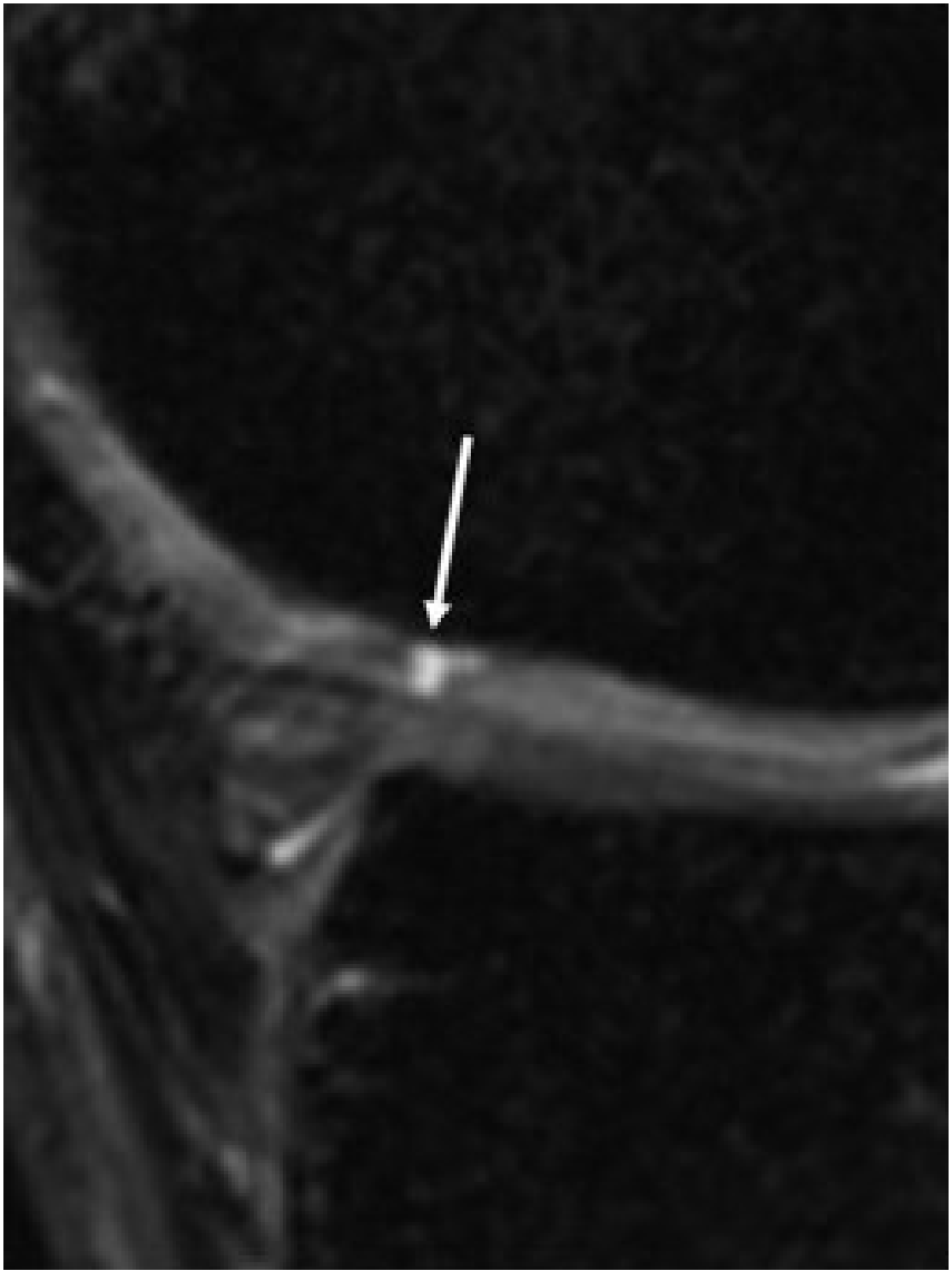

Fig 3E

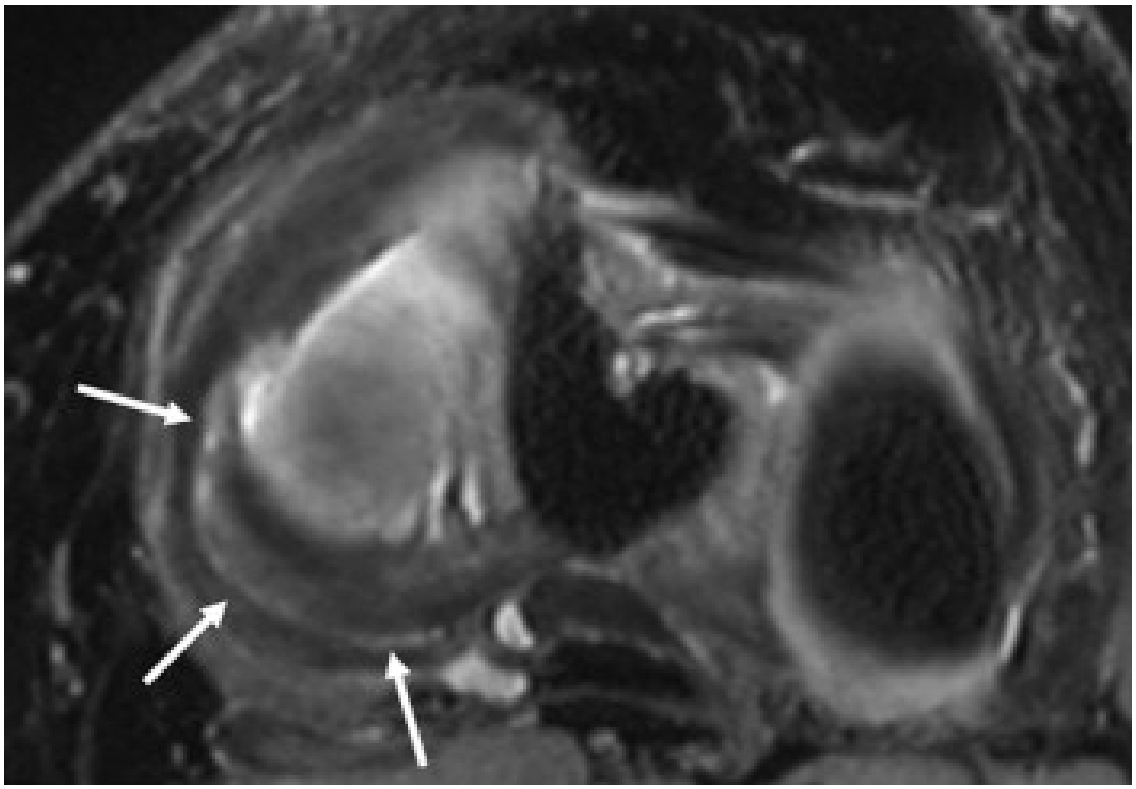

Fig 4A

Fig 4B

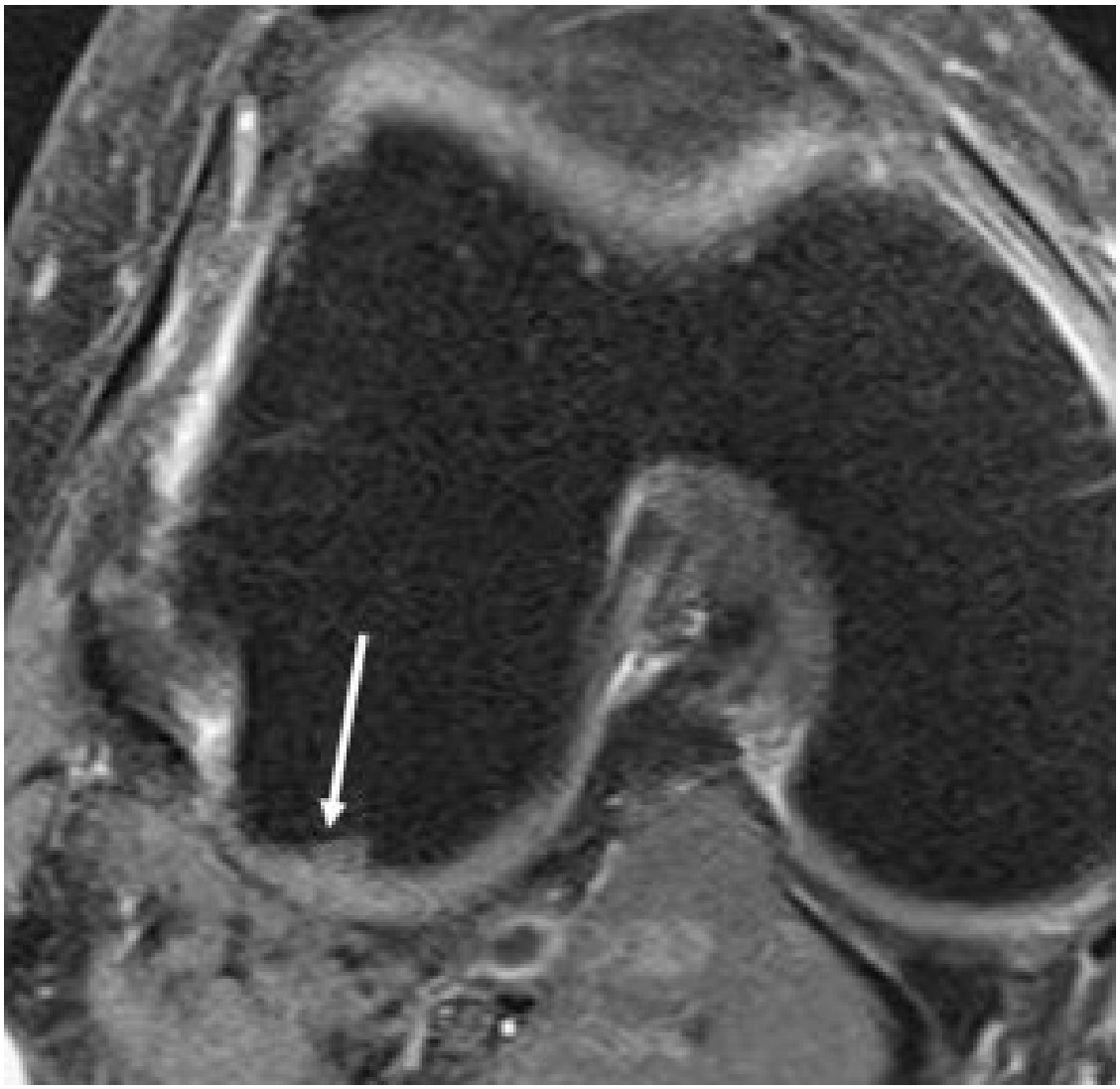

Fig 4C

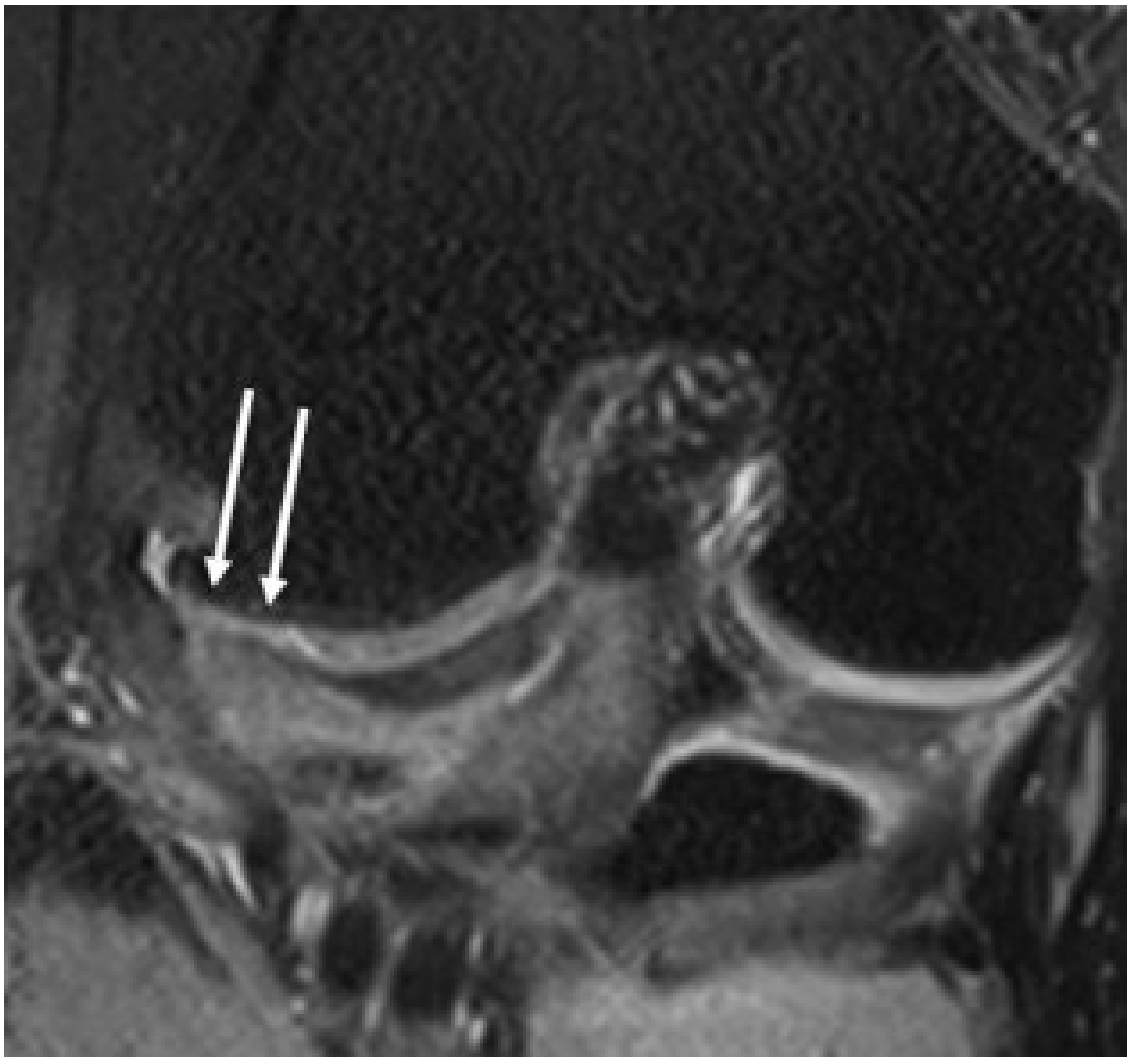

Fig 4D

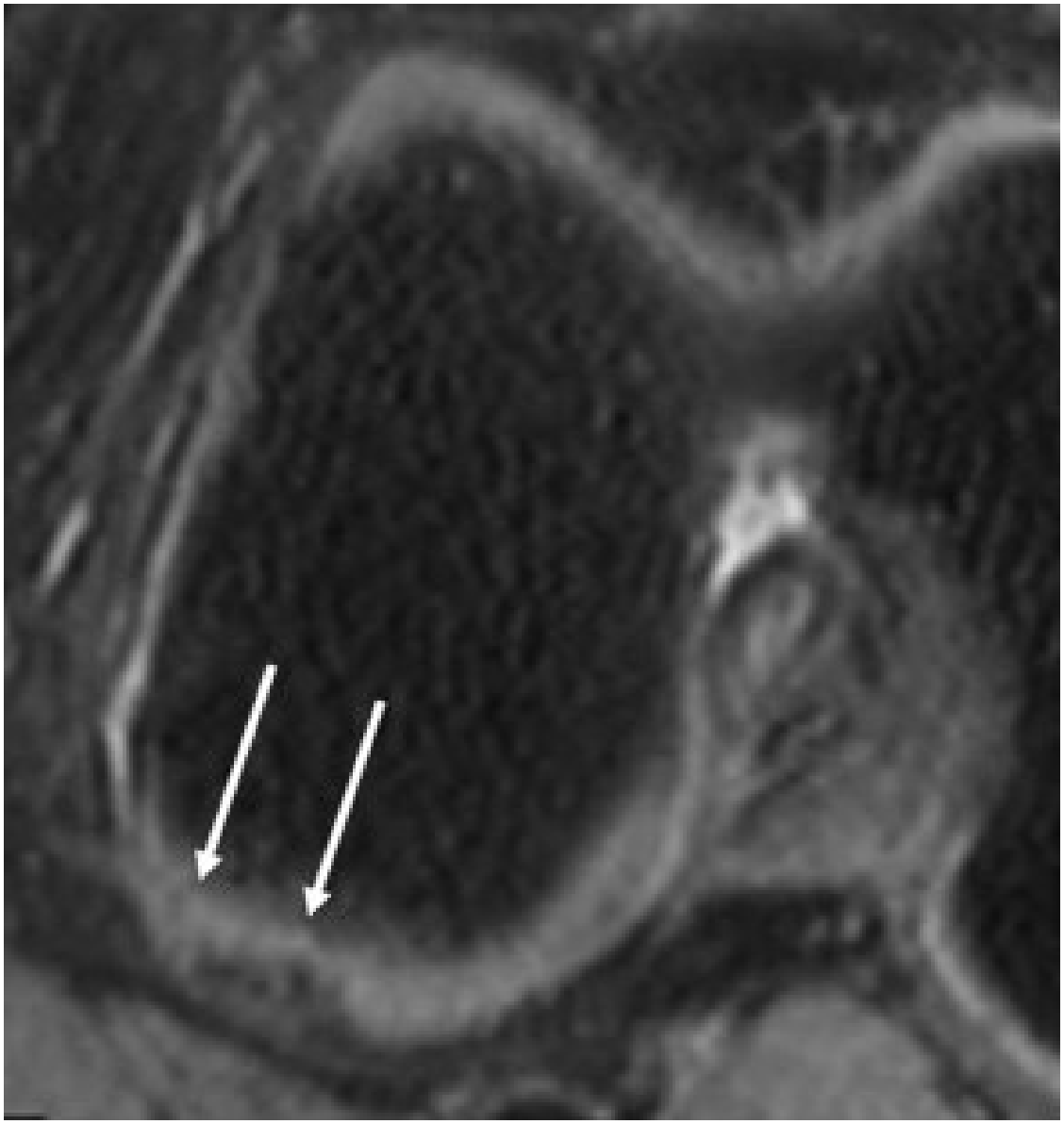

Fig 5A

Fig 5B

Fig 5C